Superlattices and Microstructures, Vol. 25, No. 1/2, 1999
Article No. spmi.1998.0646
Available online at http://www.idealibrary.com on IDEAL

A nonlinear transport device with no intrinsic threshold

A. M. SONG†, S. MANUS, M. STREIBL, A. LORKE, J. P. KOTTHAUS
Center for NanoScience and Sektion Physik der LMU, Geschwister-Scholl Platz 1, 80539 München, Germany
W. WEGSCHEIDER, M. BICHLER
Walter-Schottky-Institut der TUM, 85748 Garching, Germany

(Received 26 October 1998)

A ballistic rectifier, based on guidance of carriers by a triangular antidot, is shown to be both experimentally and theoretically capable of operating for weak signals. At $T = 4.2$ K, we find that the ballistic rectifier works when the input voltage is as low as 0.5 mV, the same order of k_BT. Based on an extended Landauer–Büttiker formula for nonlinear transport, we show that even when the input signal is much smaller than k_BT, temperature has no obvious influence on the rectification effect.

Key words: nonlinearity, ballistic transport, rectification, threshold.

There is increasing attention paid to nonlinear ballistic transport both experimentally [1–5] and theoretically [6–11]. Nonlinearity is important in mesoscopic conductors because of the small device feature sizes and the fact that in principle nonlinearity starts at any nonzero current. Recently, nonlinear ballistic transport in a semiconductor microjunction, where an antidot guides carriers to a predetermined direction, was studied [12]. A new rectification phenomenon was among the observed striking geometric effects. It was argued that the so-called ballistic rectifier has no intrinsic threshold.

Here, we perform ac measurements up to 10 GHz to study the response of the ballistic rectifier to weak signals down to 0.5 mV, which is of the same order as k_BT at 4.2 K. We then develop a model to describe quantitatively the response of the device to signals much smaller than k_BT.

The device is fabricated on a GaAs/AlGaAs heterostructure with a two-dimensional electron gas of carrier density $5 \times 10^{11}\text{cm}^{-2}$ and mobility $5 \times 10^5\text{cm}^2\ \text{V}^{-1}\text{s}^{-1}$ at 4.2 K. Figure 1A schematically shows the central part of the device where the dark areas are etched. The four channels of the cross junction are labeled as S (source), D (drain), U (upper), and L (lower). The arrows in Fig. 1A represent typical trajectories of electrons ejected from S or D, and illustrate that a positive voltage might be induced between U and L because of the guidance of carriers by the triangular antidot. We point out that the above picture is only correct in the nonlinear transport regime [12]. The square dots in Fig. 1B represent the output dc voltages measured between U and

†Present address: Solid State Physics, Lund University, 22100 Lund, Sweden. E-mail: aimin.song@ftf.lth.se

0749–6036/99/010269 + 04 $30.00/0

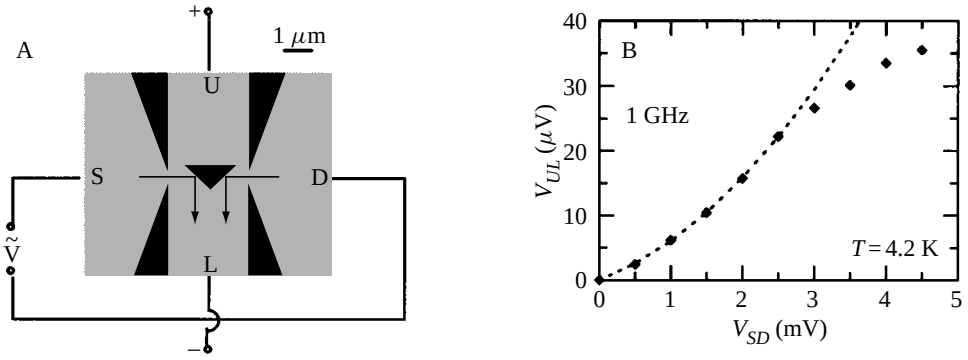

Fig. 1. A, Schematic diagram of the central part of a ballistic rectifier, where the dark areas are etched down. The arrows represent typical trajectories of electrons ejected through S and D. B, The square dots represent the measured dc voltage V_{UL} as a function of the ac voltage V_{SD} at frequency 1 GHz. The experimental result is well-fitted by the parabolic dashed line at low voltages.

L, V_{UL}, as a function of the input ac voltage between S and D, V_{SD}, at 4.2 K[†]. A custom-built electronic filter is used to determine reliably the dc component of the output voltage between U and L, V_{UL}. The frequency of the input signal is fixed at 1 GHz. As expected, the device produces positive dc voltages V_{UL}. Clearly, we find that the device operates even at $V_{SD} = 0.5$ mV, which is of the same order as $k_B T$.

We also measure the frequency response of the ballistic rectifier. Figure 2 plots the dc output voltage V_{UL} as a function of the frequency, of the applied ac voltage (fixed at 5 mV) ranging from 1 GHz to 10 GHz. Below 1 GHz, we have found that there is no decrease of the rectification efficiency with increasing frequency of the input signal. Here, however, V_{UL} decreases when the frequency is above 2 or 3 GHz. In addition, the curve exhibits fluctuations. We point out that the experimental setup used for this measurement has not been optimized yet. In a separate test on the setup (without the device), the transmission through the sample holder and the chip-carrier is indeed found to decrease with frequency and to have similar fluctuations. This suggests that the decreasing of V_{UL} with frequency in Fig. 2 most likely results from the unoptimized experimental setup, which causes the real voltage drop on the sample to be less than the output voltage of the signal source. The ballistic rectifier is expected to be able to operate at very high frequencies because of the low in-plane capacitance and the ballistic transport nature. Currently, microwave (∼100 GHz) and far-infrared (∼THz) measurements on specially designed devices are in progress.

In Ref. [13], we have shown that in the limit of $T = 0$, the ballistic rectifier works at any nonzero input voltage or current. It is of practical interest to check if a finite temperature will smear out the rectification effect when input voltages are smaller than $\frac{k_B T}{e}$. Similar to Ref. [13], we start from the expression of the electric current through lead α of the ballistic rectifier,

$$I_\alpha = \frac{2e}{h} \sum_\beta \int [\, f(E - \mu_\alpha) T_{\beta \leftarrow \alpha}(E, B, \{\mu_\gamma\}) - f(E - \mu_\beta) T_{\alpha \leftarrow \beta}(E, B, \{\mu_\gamma\})] \, dE. \tag{1}$$

Here, $f(E - \mu_\alpha) = [\exp(\frac{E - \mu_\alpha}{k_B T}) + 1]^{-1}$ is the Fermi–Dirac distribution function and μ_α is the chemical potential deep inside the contact (carrier reservoir) α. The total transmission coefficient for carriers from lead α to lead β, $T_{\beta \leftarrow \alpha}(E, B, \{\mu_\gamma\})$, is a function of energy E, magnetic field B, and the self-consistent field in

[†]In fact, there is another similar device fabricated simultaneously on the same Hall bar as the present device. So, the actual voltage across each device is only about half of the input voltage, or, strictly speaking, slightly less than that because of the resistances of the ohmic contacts. Throughout the paper, we refer V_{SD} to the half of the applied ac voltage across the whole Hall bar for simplicity. In addition, to account for the spurious thermal voltage, the curves displayed here have been offset vertically by a small constant amount.

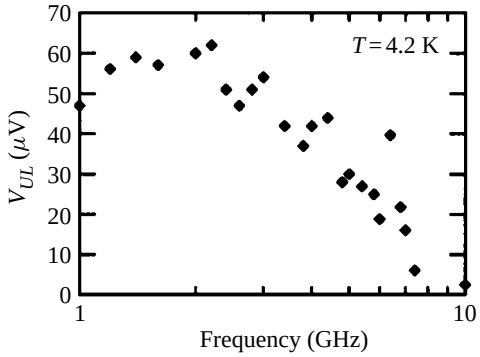

Fig. 2. The dc output voltage V_{UL} as a function of the frequency of the input signal fixed at 5 mV.

the device determined by all the chemical potentials of the contacts denoted by $\{\mu_\gamma\}$. We shall discuss the case when the applied voltages are much smaller than $\frac{k_B T}{e}$ while $k_B T$ is much lower than the Fermi energy, E_F, i.e. $|\mu_\alpha - \mu_\beta| \ll k_B T \ll E_F$. At $T = 4.2$ K, for example, $k_B T \approx 0.36$ meV while $E_F \approx 18$ meV for the present device.

Because of the Fermi–Dirac distribution functions in eqn (1), one only needs to evaluate the integral in the interval between $(\mu_\alpha - nk_B T)$ and $(\mu_\alpha + nk_B T)$ where $n \gg 1$. In such an interval, one can, to a good approximation, assume that $T_{\beta\leftarrow\alpha}(E, \{\mu_\gamma\})$ is a linear function of E. Using $f(E - \mu_\alpha) - f(E - \mu_\beta) \approx -(\mu_\alpha - \mu_\beta)\frac{\partial f}{\partial E}$, eqn (1) is reduced to

$$I_\alpha \approx \frac{2e}{h} \sum_\beta T_{[\beta,\alpha]}(\{\mu_\gamma\})(\mu_\alpha - \mu_\beta), \tag{2}$$

where $T_{[\beta,\alpha]}(\{\mu_\gamma\})$ equals $T_{\beta\leftarrow\alpha}$ at μ_α if $\mu_\alpha > \mu_\beta$ or $T_{\alpha\leftarrow\beta}$ at μ_β otherwise, reflecting the direction of net flow of carriers.

To obtain the relation between V_{UL} and V_{SD}, one needs to evaluate the two-terminal resistance $R_{SD} \equiv \frac{V_{SD}}{I_{SD}}$. It can be shown that $R_{SD} \approx \frac{h}{e^2}\frac{1}{N_{SD}}$ in the weakly nonlinear transport regime. R_{SD} only depends on the number of propagating modes in lead S or D, N_{SD}, not that in lead L or U, N_{LU}. Therefore, in analogy with the calculation in Ref. [13], we find

$$V_{UL} \approx \frac{3e}{8\pi E_F} \frac{N_{SD} \sin 2\theta_0}{2N_{LU} - 3N_{SD}(1 - \sin\theta_0)^2} V_{SD}^2, \tag{3}$$

where $\theta_0 \approx \frac{\pi}{4}$ is determined by the device geometry.

We note that there is no term of temperature T in eqn (3), which means that the rectification efficiency is independent of temperature even when the input signal is much lower than $k_B T$, i.e. temperature will not smear out the ballistic rectification effect as long as the temperature is not high enough to affect the ballistic nature of the transport. The I–V characteristic of a p–n diode has a very strong temperature dependence because it relies on minority carriers, the density of which strongly depends on $k_B T$. Our device, however, does not rely on minority carriers and is thus insensitive to temperature. Therefore, similar to tunneling diodes such as backward diodes, the ballistic rectifier is especially suitable for low noise measurements as it can be cooled to reduce noise. From eqn (3), we also notice a quadratic response of V_{UL} to input signal, which is quite different from the exponential response of a normal diode. In agreement with this result, we find that the data in Fig. 1B can be well fitted by a parabolic curve (the dashed line) at low input voltages (the apex of the parabolic fitting curve is shifted away from $V_{SD} = 0$, the ideal case expected from eqn (3), most likely because of the spurious thermal voltages or currents). This characteristic is favorable for the detection of

weak signal, as the output voltage of this device is not reduced dramatically with decreasing magnitude of the input signals. We note that both advantages are intrinsic to the working principle itself rather than achieved by precisely controlling the material parameters such as doping levels or interface properties.

There also exist shortcomings of the present device. We find that the rectification efficiency in Fig. 1B is only about 1 percent. However, this can be substantially improved by, for example, using a top gate to lower the Fermi level, or using better designed device geometries which tailor the relevant parameters in eqn (3). Another disadvantage is the need for ballistic transport. This device has to be cooled below 77 K. Nevertheless, as smaller and smaller devices can be fabricated nowadays, the ballistic rectification effect is expected to be realized at higher and higher temperatures.

Finally, we wish to point out that the ballistic rectification effect might be in analogy with, or even related to, the so-called photogalvanic effect—dc current or voltage induced in homogeneous crystals by uniform illumination [14]. To explain the photogalvanic effect, the asymmetry of elastic scattering centers was pointed out to be a key reason. For a scattering potential which lacks central symmetry, the transition probability of a particle from a state with momentum k to another state k', $W_{k'\leftarrow k}$, may differ from that from $-k$ to $-k'$, i.e. $W_{k'\leftarrow k} \neq W_{-k'\leftarrow -k}$. In this device, for instance, an electron moving from left to right in lead S with momentum $k_{\rightarrow}$ will be reflected by the antidot to L with momentum $k_{\downarrow}$, while an electron in lead D with momentum $k_{\leftarrow} = -k_{\rightarrow}$ will also be reflected to L with $k_{\downarrow}$ rather than moving upwards with momentum $k_{\uparrow} = -k_{\downarrow}$.

Acknowledgements—We acknowledge our enlightening discussions with A. Wixforth and A. Haubrich and wish to thank M. Büttiker, J. H. Davies, R. Landauer, and L. I. Magarill for helpful correspondence. A. M. S. is supported by the Alexander von Humboldt Foundation. This work is supported through a Max-Plank Research Award, Deutsche Forschungsgemeinschaft (SFB 348), and BMBF under grant 01BM623.

References

[1] A. Palevski, C. P. Umbach, and M. Heiblum, Appl. Phys. Lett. **55**, 1421 (1989).
[2] R. Taboryski, A. K. Geim, M. Persson, and P. E. Lindelof, Phys. Rev. **B49**, 7813 (1994).
[3] R. I. Hornsey, A. M. Marsh, J. R. A. Cleaver, and H. Ahmed, Phys. Rev. **B51**, 7010 (1995).
[4] D. R. S. Cumming and J. H. Davies, Appl. Phys. Lett. **69**, 3363 (1996).
[5] A. Messica, A. Soibel, U. Meirav, Ady Stern, Hadas Shtrikman, V. Umansky, and D. Mahalu, Phys. Rev. Lett. **78**, 705 (1997).
[6] R. Landauer, *Nonlinearity in Condensed Matter*, edited by A. R. Bishop, D. K. Campbell, P. Kumar, and S. E. Trullinger (Springer, Berlin, 1987).
[7] H. van Houten and C. W. J. Beenakker, *Nanostructure Physics and Fabrication*, edited by M. A. Reed and W. P. Kirk (Academic Press, New York, 1989).
[8] P. F. Bagwell and T. P. Orlando, Phys. Rev. **B40**, 1456 (1989).
[9] L. I. Glazman and A. V. Khaetskii, Europhys. Lett. **9**, 263 (1989).
[10] T. Christen and M. Büttiker, Europhys. Lett. **35**, 523 (1996).
[11] S. Ulreich and W. Zwerger, Superlattices Microstruct. **23**, 719 (1998).
[12] A. M. Song, A. Lorke, A. Kriele, J. P. Kotthaus, W. Wegscheider, and M. Bichler, Phys. Rev. Lett. **80**, 3831 (1998).
[13] A. M. Song, Phys. Rev. **B** (in press).
[14] See, for example, Fig. 3 and eqn (1.2) in V. I. Belinicher and B. I. Sturman, Sov. Phys. Usp. **23**, 199 (1980).